

Supplement of Atmos. Chem. Phys., 16, 6027–6040, 2016
<http://www.atmos-chem-phys.net/16/6027/2016/>
doi:10.5194/acp-16-6027-2016-supplement
© Author(s) 2016. CC Attribution 3.0 License.



Atmospheric
Chemistry
and Physics
Open Access
EGU

Supplement of

Effect of varying experimental conditions on the viscosity of α -pinene derived secondary organic material

James W. Grayson et al.

Correspondence to: Allan K. Bertram (bertram@chem.ubc.ca)

The copyright of individual parts of the supplement might differ from the CC-BY 3.0 licence.

Supplemental Information

1 Effect of carrier gas flow on SOM particle properties

To determine whether particles evaporate whilst being exposed to a flow of N₂ gas, a sample (generated with a mass concentration of 6,000 μg m⁻³) was mounted in the flow cell and exposed to dry (<0.5 % RH) N₂ gas for a period of 45 h. A series of nine images were taken of each of five particles over a time period of 45 h. The area at the particle-substrate interface of each particle was measured using Leica software, and equilibrium contact angle measurements of particles in the sample were made after the completion of the experiment. From this information, the volume of each of the particles was determined at each time point, with the equilibrium contact angle assumed to remain constant during the duration of the experiment. To remove the potential of photo-induced changes to the sample the light source was only turned on when acquiring images. Poke-flow experiments were also performed after 1 h and 45 h of exposure to the dry N₂ gas flow to determine whether the viscosity of the particles changed due to the extended exposure. The results of these studies are shown in Figure S1 and Table S1.

We estimate the maximum expected increase in viscosity of the SOM during exposure to a dry N₂ gas flow by assuming we have a two component system and using the equation for mixtures suggested by Arrhenius,

$$\eta_{mix} = \chi_a \ln(\eta_a) + \chi_b \ln(\eta_b) \quad (1)$$

, where a and b are the two components, χ represents the mole fraction of each component in the mixture (mix), and η represents viscosity. To take an extreme case, we assumed at a time of 1 hour (the start of the experiment) the first component, a, is non-volatile and the second component, b, is volatile and of viscosity similar to that of water (10⁻³ Pa s). We assume at 45 hours (the end of the experiment) all of component b has evaporated, and therefore $\chi_a = 1$ and $\chi_b = 0$. We also assume that at 1 hour, $\chi_b \leq 0.065$ (which is the maximum possible value of χ_b based on the uncertainty in the optical images and assuming component b had completely evaporated after 45 hours), making $\chi_a \geq 0.935$ (1 - 0.065).

At a time of 1 hour, the measured viscosity (η_{mix}) was 6.4 x 10⁵ Pa s, and hence based on the Arrhenius mixing rule (equation S1, above) and the assumptions above, $\eta_a \leq 2.6 \times 10^6$ Pa s. Assuming $\chi_a = 1$ after 45 hours produces an upper limit for η_{mix} after 45 hours of 2.6 x 10⁶ Pa s, consistent with the viscosity measured (1.0 x 10⁶ Pa s). Hence the evaporation of a semi-volatile component combined with the Arrhenius mixing rule during the 44 hours of exposure is consistent with the small increase in viscosity observed in the experiments. The values of η and χ discussed in this paragraph are summarised in Table S2.

2 Variability between particles in the same sample, and between all particles produced under equivalent conditions

To determine the variability in $\tau_{exp,flow}$ and the variability in the simulated lower and upper limits of viscosity for particles produced using equivalent conditions, the percent relative standard deviations (% RSD) have been calculated for poke-flow experiments performed at <0.5 % RH, and are reported in Table S5.

Table S5 shows the % RSD for all particles produced under equivalent conditions ranged from 26-117 %. For samples on the same substrate, the % RSD ranged from 14-83 %. In general there appears to be a reasonable level of reproducibility in results both between particles on the same substrate, and between particles on separate substrates produced under equivalent conditions. The majority of the uncertainty in the reported viscosities is due to uncertainty in the physical parameters

45 used during simulations, rather than experimental variability or error, as can be seen in Figs. 3b, 5b,
& S3b.

3 Calculation of limits of viscosity from previous studies of SOM produced via the ozonolysis of α -pinene

Saleh et al. (2013) and Robinson et al. (2013) reported mixing times for particles of a given size,
50 which have been used to calculate diffusion coefficients through the relationship,

$$D = d_p^2 / 4\pi^2 \tau_{mixing} \quad (2)$$

where d_p is the diameter of the particle (m), and τ_{mixing} is the mixing time in s (Shiraiwa et al., 2011). The calculated diffusion coefficients for Saleh et al. (2013) and Robinson et al. (2013) should
55 be considered as lower limits, as the mixing times used were the upper limit of those reported, and
other processes besides molecular diffusion within the particles may have been the rate determining
step for mixing in their experiments. These calculated upper limits to diffusion coefficients were
then converted to lower limits of viscosities through the Stokes-Einstein relationship,

$$\eta = kT / x\pi r D \quad (3)$$

where k is the Boltzmann constant ($J K^{-1}$), T is the temperature (K), x is a coefficient ranging
60 from 4-6 dependent upon the assumption of slip or no-slip at the surface of the diffusing species,
and r is the hydrodynamic radius of the diffusing molecule (m). A summary of the values used to
calculate viscosities is included in Table S6.

As the size of the diffusing molecules were not known in Saleh et al. (2013) and Robinson et al.
(2013), we assumed a hydrodynamic radius of 0.38 nm, which corresponding to the radii of a sym-
65 metrically spherical molecule of molar mass 175 g mol^{-1} (Huff-Hartz, 2005) and density 1.3 g cm^{-3}
(Chen and Hopke, 2009). Further, x has been given a value of 4, to give conservative upper limits to
viscosity.

Abramson et al. (2013) determined the diffusion coefficient for pyrene molecules in particles of
SOM generated via the ozonolysis of α -pinene. The hydrodynamic radius of pyrene is 0.4 nm, whilst,
70 as suggested by Abramson et al. (2013) pyrene may form clusters consisting of up to 1000 molecules,
with a 1000 molecule cluster having a radius of ≈ 4 nm. Hence, when calculating viscosity using
Equation S2, from the studies of Abramson et al., we used $r = 0.4$ to 4 nm. Further, we used $x = 4-6$
in Equation 2 to calculate conservative lower and upper limits of viscosity.

Cappa and Wilson (2011) observed the change in chemical composition of SOM particles pro-
75 duced via the ozonolysis of α -pinene as the particles were heated, and conservatively estimated an
upper limit of diffusion coefficient for the particles. A value of $x = 6$ has been used in Equation S2,
along with a value of $r = 4$ nm, in order to determine a lower limit of viscosity.

Perraud et al. (2012) studied the particulate nitrate concentration in SOM particles generated via
the ozonolysis of α -pinene and determined an upper limit for the diffusion coefficient of the particles.
80 A value of $x = 6$ has been used in Equation S2, along with a value for r of 4 nm, in order to determine
a lower limit of viscosity.

4 Studies using the poke-and-flow technique combined with simulations of fluid flow for particles that exhibited cracking behaviour

In some cases (for the water-soluble SOM at low RH) the needle did not penetrate the particle.
85 Instead, the needle caused the particle to 'crack', resulting in sharp, defined edges in the SOM (see
Figure 6, panel b2 for an example). In cases where cracking occurred, the material was observed for
an extended period of time (at least 12 h). If, over that time, the sharp, defined, edges exhibited no
detectable movement, the observation time was taken as a lower limit of $\tau_{exp,flow}$.

90 Particles that exhibited cracking behaviour and no detectable flow over the course of an experiment
were simulated using a particle of quarter-sphere geometry, with one flat surface in contact with a
solid substrate (see Figure S4b and Movie S5 in Renbaum-Wolff et al. (2013)). The bottom surface,
which represented the material-substrate interface, was allowed to undergo free deformation in the
horizontal plane. All other surfaces were allowed to undergo free deformation in all directions. In
95 these simulations the viscosity of the particle was varied until the sharp edge at the top of the particle
moved by $0.5 \mu\text{m}$ over the experimental time. A value of $0.5 \mu\text{m}$ was chosen because this amount of
movement is a clearly detectable threshold for the microscopy. Thus, for experiments for which no
detectable movement was observed in microscope images, the viscosity determined via this method
is a lower limit. The values of density, particle-substrate slip length, surface tension, and contact
angle used when simulating the lower limit of viscosity for these particles are detailed in Table S7.

100 References

- Abramson, E., Imre, D., Beránek, J., Wilson, J., and Zelenyuk, A.: Experimental determination of chemical diffusion within secondary organic aerosol particles., *Phys. Chem. Chem. Phys.*, 15, 2983–2991, doi:10.1039/c2cp44013j, 2013.
- 105 Cappa, C. D. and Wilson, K. R.: Evolution of organic aerosol mass spectra upon heating: implications for OA phase and partitioning behavior, *Atmos. Chem. Phys.*, 11, 1895–1911, doi:10.5194/acp-11-1895-2011, 2011.
- Chen, X. and Hopke, P. K.: Secondary organic aerosol from α -pinene ozonolysis in dynamic chamber system, *Indoor Air*, 19, 335–345, doi:10.1111/j.1600-0668.2009.00596.x, 2009.
- Grayson, J. W., Song, M., Sellier, M., and Bertram, A. K.: Validation of the poke-flow technique combined with simulations of fluid flow for determining viscosities in samples with small volumes and high viscosities, *Atmos. Meas. Tech.*, 8, 2463–2472, doi:10.5194/amtd-8-877-2015, 2015.
- 110 Huff-Hartz, K. E.: Cloud condensation nuclei activation of monoterpene and sesquiterpene secondary organic aerosol, *J. Geophys. Res.*, 110, D14 208, doi:10.1029/2004JD005754, 2005.
- Perraud, V., Bruns, E. A., Ezell, M. J., Johnson, S. N., Yu, Y., Alexander, M. L., Zelenyuk, A., Imre, D., Chang, W. L., Dabdub, D., Pankow, J. F., and Finlayson-Pitts, B. J.: Nonequilibrium atmospheric secondary organic aerosol formation and growth., *Proc. Nat. Acad. Sci. U.S.A.*, 109, 2836–2841, doi:10.1073/pnas.1119909109, <http://www.ncbi.nlm.nih.gov/pmc/articles/PMC3286997/>, 2012.
- 115 Renbaum-Wolff, L., Grayson, J. W., Bateman, A. P., Kuwata, M., Sellier, M., Murray, B. J., Shilling, J. E., Martin, S. T., and Bertram, A. K.: Viscosity of α -pinene secondary organic material and implications for particle growth and reactivity, *Proc. Nat. Acad. Sci. U.S.A.*, 110, 8014–8019, doi:10.1073/pnas.1219548110, <http://www.pnas.org/content/110/20/8014.short>, 2013.
- 120 Robinson, E. S., Saleh, R., and Donahue, N. M.: Organic aerosol mixing observed by single-particle mass spectrometry., *J. Phys. Chem. A*, 117, 13 935–13 945, doi:10.1021/jp405789t, 2013.
- Saleh, R., Donahue, N. M., and Robinson, A. L.: Time scales for gas-particle partitioning equilibration of secondary organic aerosol formed from alpha-pinene ozonolysis., *Environ. Sci. Technol.*, 47, 5588–5594, doi:10.1021/es400078d, 2013.
- 125 Shiraiwa, M., Ammann, M., Koop, T., and Pöschl, U.: Gas uptake and chemical aging of semisolid organic aerosol particles., *Proc. Nat. Acad. Sci. U.S.A.*, 108, 11 003–11 008, doi:10.1073/pnas.1103045108, <http://www.ncbi.nlm.nih.gov/pmc/articles/PMC3131339/>, 2011.
- Tuckermann, R. and Cammenga, H. K.: The surface tension of aqueous solutions of some atmospheric water-soluble organic compounds, *Atmos. Environ.*, 38, 6135–6138, 2004.
- 130 Zhang, Y., Sanchez, M. S., Douet, C., Wang, Y., Bateman, A. P., Gong, Z., Kuwata, M., Renbaum-Wolff, L., Sato, B. B., Liu, P. F., Bertram, A. K., Geiger, F. M., and Martin, S. T.: Changing shapes and implied viscosities of suspended submicron particles, *Atmos. Chem. Phys.*, 15, 7819–7829, doi:10.5194/acpd-15-7783-2015, 2015.

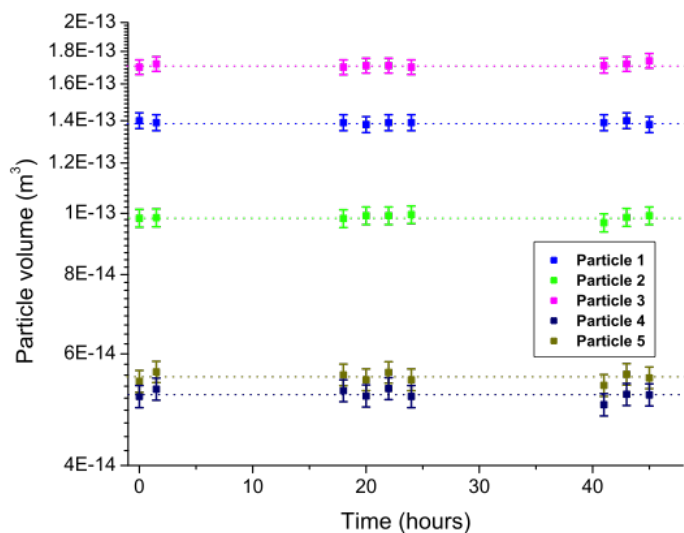


Figure 1. A plot of particle volume vs. time for five particles exposed to a dry ($<0.5\%$ RH) N_2 gas flow. Dotted lines represent the measured mean size of a particle. Error bars on the y-axis represent the uncertainty in measuring both the area of the particle, and the equilibrium contact angle, at the particle-substrate interface.

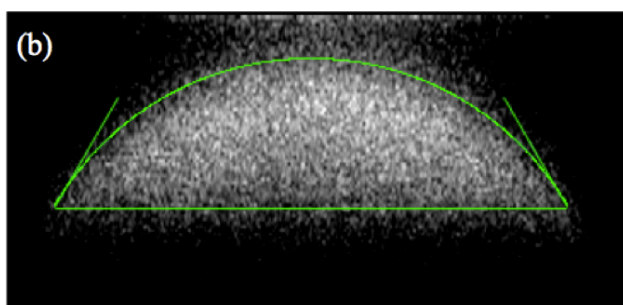
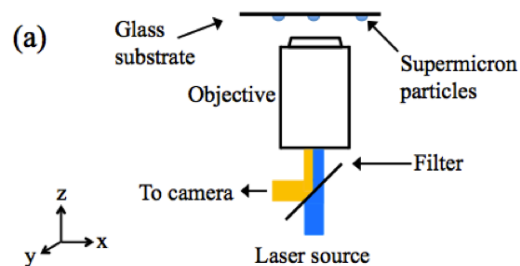


Figure 2. (a) Schematic representation of instrumental setup for contact angle images. (b) Fluorescence image obtained of an SOM particle. The green overlay is used to determine the contact angle of the particle, in this case 60° , and was produced using the LB-ADSA plugin for ImageJ.

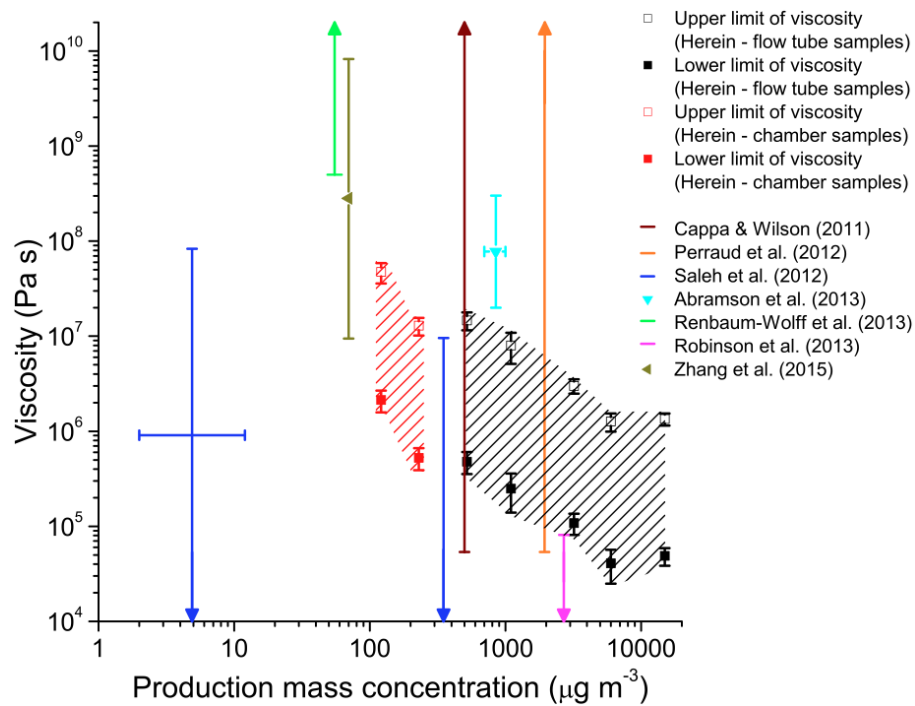


Figure 3. Plot of production mass concentration vs. viscosity for whole SOM produced via the ozonolysis of α -pinene and studied at <5 % RH. Shown are the results determined here along with those previously reported in literature (Cappa and Wilson, 2011; Perraud et al., 2012; Saleh et al., 2013; Abramson et al., 2013; Renbaum-Wolff et al., 2013; Robinson et al., 2013; Zhang et al., 2015).

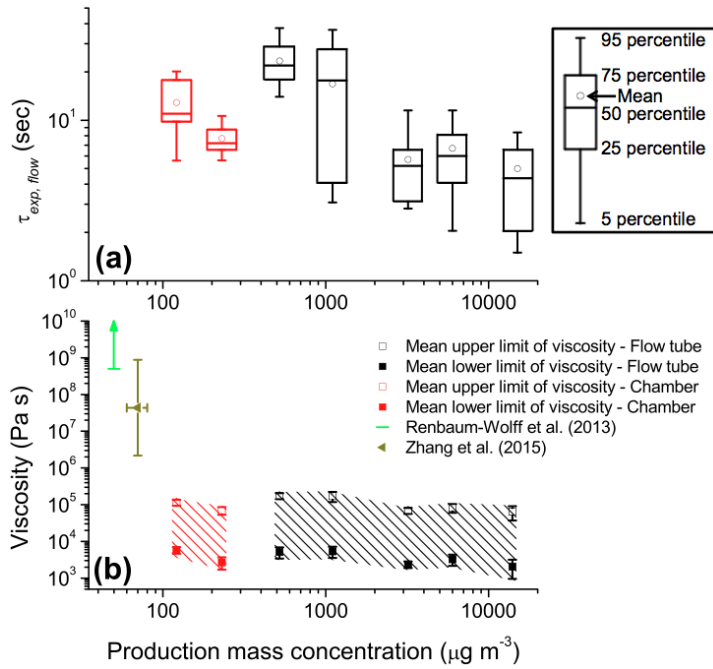


Figure 4. Summary of poke-flow experiments performed on particles of whole SOM at 30 % RH. Black symbols represent results from particles produced in a flow tube, whilst red symbols represent results from particles produced in a chamber. Panel (a) shows box plots of observed $\tau_{exp,flow}$ times at different SOM mass concentrations for particles studied using the poke-and-flow at 30 % RH. Boxes represent the 25, 50, and 75 percentiles, open circles represent median values, and whiskers represent the 5 and 95 percentiles. Panel (b) shows the simulated lower (filled squares) and upper (open squares) limit of viscosity for particles at each SOM mass concentration studied using the poke-and-flow technique at 30 % RH. Symbols represent mean values, whilst the y error bars represent 95 % confidence intervals. The shaded region is included to guide the eye of the reader. Also included in (b) are literature viscosities from Renbaum-Wolff et al. (2013) and Zhang et al. (2015), for SOM produced via the ozonolysis of α -pinene and studied at 30 % RH.

Table 1. Summary of $\tau_{exp,flow}$ times and viscosities of sample analysed after both 1 hour and 45 hours of exposure to a dry (<0.5 % RH) flow of Nitrogen gas.

Exposure time	$\tau_{exp,flow}$ (sec) ^a	Mean simulated viscosity \pm 95 % confidence intervals (Pa s) ^b	
		Lower limit	Upper limit
1 hour	104.3 (80.3,120.5)	$1.5 \times 10^4 \pm 5.0 \times 10^3$	$6.4 \times 10^5 \pm 9.0 \times 10^4$
45 hours	107.8 (80.6, 141.1)	$3.0 \times 10^4 \pm 9.3 \times 10^3$	$1.0 \times 10^6 \pm 2.3 \times 10^5$

^a $\tau_{exp,flow}$ values represent experimental values in the form "mean (5th percentile, 95th percentile)".

Table 2. Values used during calculations of viscosity in SOM using the Arrhenius equation.

	η_{mix} / Pa s	χ_a	η_a / Pa s	χ_b	η_b / Pa s
After 1 hour	6.4×10^5 (measured)	≥ 0.935 (calculated)	$\leq 2.6 \times 10^6$ (calculated)	≤ 0.065 (calculated)	1.0×10^{-3} (assumed)
After 45 hours	1.0×10^6 (measured)	1.000 (assumed)	$\leq 2.6 \times 10^6$ (calculated)	0.000 (assumed)	N/A

Table 3. Physical parameters used when simulating particles that exhibited flow with COMSOL.

	Density (kg m^{-3}) ^a	Slip length (m) ^b	Surface tension (mN m^{-1}) ^c	Contact angle
Value used to determine lower limit of viscosity	1,300	5×10^{-9}	40	See Table S4 ^d
Value used to determine upper limit of viscosity	1,300	1×10^{-5}	75	See Table S4 ^d

^a Density was varied from 1,000 - 1,400 kg m^{-3} based on the work of Chen and Hopke (2009) and determined to have no effect upon viscosities determined via simulation. As such a median value of 1300 kg m^{-3} was used.

^b For references and rationale see Grayson et al. (2015).

^c Range of surface tension values based on work on Tuckermann and Cammenga (2004).

^d The lower value from Table S4 is used for particles of geometry $(R_0 - r_0) / r_0 < 2$, and the upper value from Table S4 is used for particles of geometry $(R_0 - r_0) / r_0 > 2$.

^e The upper value from Table S4 is used for particles of geometry $(R_0 - r_0) / r_0 < 2$, and the lower value from Table S4 is used for particles of geometry $(R_0 - r_0) / r_0 > 2$.

Table 4. Experimentally determined contact angles for each of the samples studied. The range of values represent the 95 % confidence intervals of the values measured for multiple particles.

Sample name (production mass concentration during SOM production)	Particle-substrate contact angle ($^\circ$)		
	Sample 1	Sample 2	Sample 3
Water-soluble SOM ($14,000 \mu\text{g m}^{-3}$)	43.5 - 50.0	47.2 - 53.3	50.5 - 72.0
Flow tube sample #1 ($14,000 \mu\text{g m}^{-3}$)	57.5 - 63.7	49.6 - 55.4	18.3 - 21.4
Flow tube sample #2 ($6,000 \mu\text{g m}^{-3}$)	59.8 - 61.3	60.5 - 66.9	63.3 - 67.2
Flow tube sample #3 ($3,200 \mu\text{g m}^{-3}$)	41.2 - 52.2	38.5 - 45.3	49.2 - 51.1
Flow tube sample #4 ($1,100 \mu\text{g m}^{-3}$)	31.4 - 35.6	61.5 - 65.5	44.3 - 47.8
Flow tube sample #5 ($520 \mu\text{g m}^{-3}$)	55.5 - 61.8	56.2 - 60.6	36.1 - 47.0
Chamber sample #1 ($230 \mu\text{g m}^{-3}$)	64.5 - 69.0	64.1 - 66.5	
Chamber sample #2 ($121 \mu\text{g m}^{-3}$)	60.2 - 65.1	60.7 - 80.1	

Table 5. Summary of the percent relative standard deviation (% RSD) in $\tau_{exp,flow}$, lower limits of viscosity, and upper limits of viscosity for particles produced using equivalent conditions and studied via the poke-flow technique in combination with simulations of fluid flow at <0.5 % RH. Three samples were studied per production mass concentration in the flow tube. Values prior to parentheses represent the relative standard deviation between all particles studied that were produced at a given mass concentration, whilst the values inside each parenthesis represent the average relative standard deviation between particles on the same substrate.

SOM mass particle concentration ($\mu\text{g m}^{-3}$)	% RSD of $\tau_{exp,flow}$	% RSD of simulated lower limit of viscosity	% RSD of simulated upper limit of viscosity
520	54 (30)	68 (67)	56 (39)
1,100	89 (24)	117 (44)	96 (27)
3,200	27 (22)	67 (42)	45 (30)
6,000	26 (20)	103 (47)	58 (29)
14,000	31 (27)	57 (27)	40 (28)

Table 6. Summary of parameters used to estimate viscosity from literature studies of SOM produced via the ozonolysis of α -pinene.

Reference	d_p (nm)	τ_{mixing} (sec)	x	r (nm)
Cappa and Wilson (2011)		N/A	6	4.0
Perraud et al. (2012)		N/A	6	4.0
Saleh et al. (2013) ^a	112 ^b	3,600	4	0.38
Saleh et al. (2013) ^c	38 ^b	3,600	4	0.38
Abramson et al. (2013)		N/A	4 - 6	0.4 - 4.0
Robinson et al. (2013)	>158 ^b	60	4	0.38

^a Values for experiments conducted with an SOM mass concentration of $350 \mu\text{g m}^{-3}$.

^b An aerodynamic diameter was reported, and has been converted to a geometric diameter here.

^c Values for experiments conducted with an SOM mass concentration of $1\text{-}12 \mu\text{g m}^{-3}$.

Table 7. Physical parameters when simulating particles that don't exhibit flow in COMSOL

	Density (kg m^{-3}) ^a	Slip length (m) ^b	Surface tension (mN m^{-1}) ^c	Contact angle ($^\circ$)
Value used to determine lower limit of viscosity	1,300	$1 - 1.7 \times 10^{-8}$	40	90

^a Density was varied from $1,000 - 1,400 \text{ kg m}^{-3}$ based on the work of Chen and Hopke (2009) and determined to have no effect upon simulations values. As such a median value of 1300 kg m^{-3} was used.

^b For references and rationale see Grayson et al. (2015).

^c Surface tension value based on work on Tuckermann and Cammenga (2004).